

# V-V dimerization effects on bulk-sensitive hard x-ray photoemission spectra for Magnéli phase vanadium oxides

M. Obara,<sup>1</sup> A. Sekiyama,<sup>1,2</sup> S. Imada,<sup>1,\*</sup> J. Yamaguchi,<sup>1</sup> T. Miyamachi,<sup>1</sup> T. Balashov,<sup>3</sup> W. Wulfhekel,<sup>3</sup> M. Yabashi,<sup>2,4</sup> K. Tamasaku,<sup>2</sup> A. Higashiya,<sup>2</sup> T. Ishikawa,<sup>2</sup> K. Fujiwara,<sup>5,6</sup> H. Takagi,<sup>5,6</sup> and S. Suga<sup>1,2</sup>

<sup>1</sup>Division of Materials Physics, Graduate School of Engineering Science, Osaka University, Toyonaka, Osaka 560-8531, Japan

<sup>2</sup>RIKEN, Mikazuki, Sayo, Hyogo 679-8148, Japan

<sup>3</sup>Physikalisches Institut, Karlsruhe Institute of Technology (KIT), Wolfgang-Gaede-Strasse 1, 76131 Karlsruhe, Germany

<sup>4</sup>Japan Synchrotron Radiation Research Institute, Mikazuki, Sayo, Hyogo 679-5198, Japan

<sup>5</sup>Magnetic Materials Laboratory, Discovery Research Institute, RIKEN (The Institute of Physical and Chemical Research), Wako, Saitama 351-0198, Japan

<sup>6</sup>Graduate School of Frontier Science, University of Tokyo, 5-1-5 Kashiwa, Kashiwa, Chiba 277-8561, Japan

(Received 27 December 2009; published 22 March 2010)

Highly bulk-sensitive hard x-ray photoemission has been performed for the Magnéli phase  $V_5O_9$  and  $V_6O_{11}$ , which are composed of  $V_2O_3$  and  $VO_2$  from chemical point of view. The valence-band spectra near the Fermi level are rather similar between  $V_5O_9$  and  $V_6O_{11}$  in both metallic and insulating phases. Although the core-level spectra in the metallic phase are similar between  $V_5O_9$  and  $V_6O_{11}$ , the core-level spectra in the insulating phase are noticeably different. Our results are understood by considering the contribution of the V-V dimerization effects, which are strong in  $V_6O_{11}$  and negligible in  $V_5O_9$ . Comparison of the core-level spectra of  $V_5O_9$  and  $V_6O_{11}$  with those of  $VO_2$  has revealed that the mechanism of the metal-insulator transitions for the former two compounds is different from that for  $VO_2$ .

DOI: 10.1103/PhysRevB.81.113107

PACS number(s): 71.27.+a, 71.30.+h, 79.60.-i

Among various strongly correlated electron systems, the metal-insulator transition (MIT) of vanadium oxides has been discussed for a very long time. For example, a variety of theoretical and experimental studies have been made for  $V_2O_3$  and  $VO_2$ , which show MITs as a function of temperature. In addition, it is known that structural phase transitions are associated with their MIT. Namely, corundum  $V_2O_3$  and rutile  $VO_2$  in the metallic phase show a monoclinic structure in the insulating phases.<sup>1–5</sup> While  $V_2O_3$  is thought as a typical example of the Mott-Hubbard MIT system,<sup>6</sup> the origin of the MIT in  $VO_2$  was controversial.<sup>7–14</sup> In comparison with intensive studies of MITs of  $V_2O_3$  and  $VO_2$ , the Magnéli phase vanadium oxides;  $V_nO_{2n-1}$  (with  $4 \leq n \leq 9$ ), have been less studied, though most of them show MITs as a function of temperature except for  $V_7O_{13}$ .<sup>15</sup> They show similar crystal structures<sup>16,17</sup> and can be understood to be chemically composed of  $V_2O_3$  and  $VO_2$  as  $V_nO_{2n-1} = V_2O_3 + (n-2)VO_2$ .<sup>18</sup> Metallic  $V_nO_{2n-1}$  comprises a mixture of rutile ( $VO_2$ -like) and corundum ( $V_2O_3$ -like) regions. In these  $V_nO_{2n-1}$ , crystal structures are preserved in their triclinic space group  $P\bar{1}$  across the MIT, but the lattice parameters and interatomic distances change discontinuously. Therefore, it is very important to study various  $V_nO_{2n-1}$  to understand the physics of MIT associated with the structural changes of vanadium oxides.

Photoelectron spectroscopy (PES) is a powerful tool to study the electronic structures of materials.<sup>19</sup> In the case of strongly correlated electron systems, however, the importance of bulk sensitivity has gradually been recognized as demonstrated in the soft x-ray PES,<sup>20,21</sup> because their surface electronic structures often deviate from those in the bulk. We have here performed further bulk-sensitive hard x-ray PES (Refs. 22 and 23) (HAXPES) for  $V_5O_9$  and  $V_6O_{11}$ .

The crystal structures of  $V_5O_9$  and  $V_6O_{11}$  were already described in detail by Marezio *et al.*<sup>24</sup> and Schwingenschlög

*et al.*<sup>25</sup> As schematically shown in Fig. 1, their structures are rather similar. The homologous number  $n=5$  or 6 corresponds to the length of the chains of the O octahedra with V atoms inside along the pseudorutile  $c_{prut}$  axis in the figure. In the case of rutile structure ( $VO_2$ ), these chains have infinite length and, therefore,  $VO_2$  is assumed to be the end member of  $V_nO_{2n-1}$  ( $n=\infty$ ). On the chain along the same  $c_{prut}$  axis, one can also see 4 or 5 ( $=n-1$ ) empty O octahedra without central V atoms. In the bottom panels of Fig. 1, the two adjacent chains along the  $c_{prut}$  axis with 5 and 6 filled V atoms are displayed for  $V_5O_9$  (left) and  $V_6O_{11}$  (right). There are two different types of layers for both materials. One is the layer formed by only odd-numbered vanadium atoms (V1, V3, and V5) and the other is composed of even-numbered vanadium ions (V2, V4, and V6), whose nomenclature follows Refs. 24 and 25 reflecting the site difference with different effective charges. The two layers alternate along the  $a_{prut}$  axis. In order to make connections between the V1 and V2 atoms, the vanadium chains are shifted parallel to the  $c_{prut}$  axis.<sup>25</sup> Although  $V_5O_9$  and  $V_6O_{11}$  preserve their crystal structures of  $P\bar{1}$  type across the MIT, they show a kind of structural transformation. The most significant changes take place for the distances between vanadium ions. Especially in  $V_6O_{11}$ , V4-V6 dimers are formed with changing their distances from 2.85 Å in the metallic phase to 2.62 Å in the insulating phase. Such a change is analogous to the V-V dimerization in  $VO_2$  across the MIT. In contrast, there is little change in the V-V distances across the MIT for  $V_5O_9$ .<sup>24</sup> Then, we can regard  $VO_2$ ,  $V_5O_9$ , and  $V_6O_{11}$  as fully dimerized, nondimerized, and partially dimerized systems, respectively.

The samples employed here were single-crystalline  $V_5O_9$  and  $V_6O_{11}$  grown by chemical-vapor transport using  $TeCl_4$ .<sup>26</sup> HAXPES measurements were performed at BL19LXU of SPring-8.<sup>27</sup> The spectra were measured with the MBS A1-HE

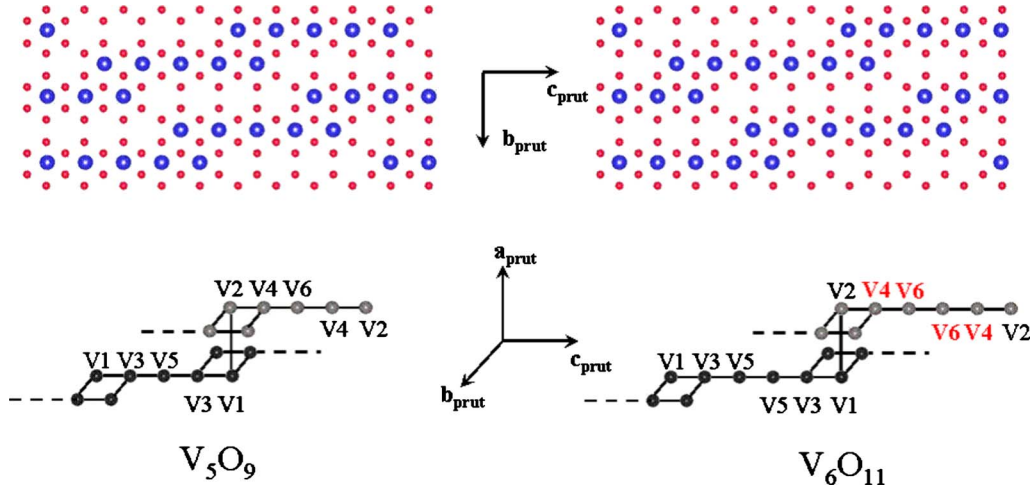


FIG. 1. (Color online). Schematic crystal structure of  $V_5O_9$  (left) and  $V_6O_{11}$  (right). Top two panels are viewed along the  $a_{prut}$ . Large open and small filled circles mark vanadium and oxygen atoms, respectively. The hexagonal arrangement of O atoms does not show the real position of the O atoms but only stands for the O octahedron. Bottom two panels are schematic views of two adjacent V chains along the  $a_{prut}$  axis.

analyzer. The photon energy  $h\nu$  was set to  $\sim 7945$  eV so that enough bulk sensitivity can be realized even in such a deep binding energy ( $E_B$ ) region as the V  $1s$  core level. Clean surfaces were obtained by fracturing *in situ* under  $\sim 4.0 \times 10^{-8}$  Pa. The Fermi energy ( $E_F$ ) was calibrated by the Fermi edge of Au electrically connected to the sample. The total energy resolution was set to about 180 meV. Because the MIT temperature  $T_i$  for  $V_5O_9$  ( $V_6O_{11}$ ) is about 135 K (Refs. 24, 28, and 29) [170 K (Refs. 25 and 30)], measurements in the metallic phase were first performed at 150 K (200 K). Then, spectra in the insulating phase were measured at 100 K (150 K).

Figure 2 displays valence-band HAXPES spectra of  $V_5O_9$  and  $V_6O_{11}$  in both metallic (upper two spectra: M) and insulating (lower two spectra: I) phases. MITs are clearly observed in both  $V_5O_9$  and  $V_6O_{11}$  by comparing the spectra in the metallic and insulating phases. It should be noticed that the spectral shapes are rather similar between  $V_5O_9$  and  $V_6O_{11}$  in both phases. In the metallic phase a prominent coherent peak (quasiparticle) is clearly observed in both materials, which crosses  $E_F$  with noticeable intensity. In addition, incoherent parts corresponding to the lower Hubbard band (LHB) are observed as a tail or weak shoulder in the higher  $E_B$  region (labeled L) between  $\sim 1$  and  $\sim 2$  eV. The incoherent parts are also observed in the insulating phase between 1.5 and 2.6 eV as a characteristic tail of the peak located at  $\sim 0.7$  ( $\sim 0.8$  eV) in  $V_5O_9$  ( $V_6O_{11}$ ).<sup>31</sup> Note that this strong peak in the insulating phase is located at much lower  $E_B$  than that of the LHB in the metallic phase. Therefore the peak at 0.7–0.8 eV in the insulating phase cannot be simply interpreted as LHB but should be interpreted as reflecting coherent spectral weight. Such a situation was suggested from the dynamical mean-field theory for insulating  $3d^1$  transition-metal oxides.<sup>13,32</sup> Although the V  $3d$  valence band spectrum in the insulating phase of  $V_2O_3$  is interpreted as  $3d^2\bar{L}$  single component ( $\bar{L}$  is a ligand hole) in Ref. 33, the multiple component structures must be considered for a proper analysis.

While the spectral shape near  $E_F$  does not show promi-

nent difference between  $V_5O_9$  and  $V_6O_{11}$ , significant changes are observed in the core-level spectra. As the first example, the V  $1s$  core-level spectra are shown in Fig. 3(a). After the subtraction of an integral background, each spectrum is normalized by the integrated intensity of the V  $1s$  main peak. On the lower  $E_B$  side of the main peak, one can recognize in each metallic phase a shoulder structure labeled A. It is ascribed to the well-screened final states where the core holes are screened by conduction electrons. Such a feature is absent in the spectra of the insulating phase. A similar structure in the core-level spectra has been reported not only

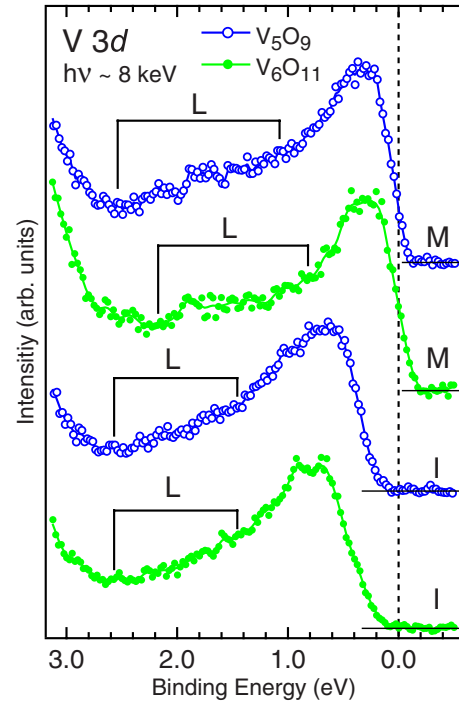


FIG. 2. (Color online). Valence-band spectra of  $V_5O_9$  (spectra with open  $\circ$  mark) and  $V_6O_{11}$  (spectra with filled  $\bullet$  mark). Upper (lower) two spectra are in the metallic: M (insulating: I) phase. The solid lines show the smoothed data.

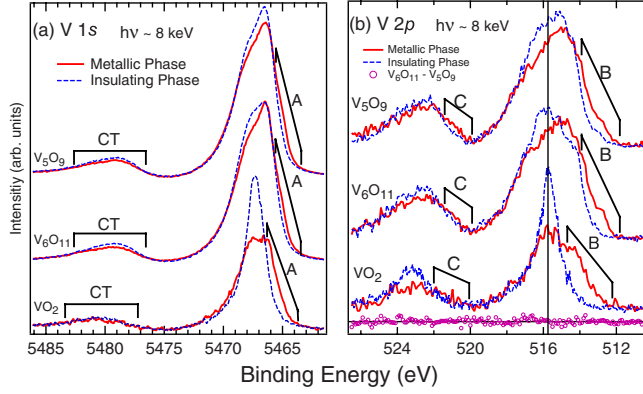


FIG. 3. (Color online). (a) V  $1s$  and (b) V  $2p$  core-level spectra of  $V_5O_9$ ,  $V_6O_{11}$ , and  $VO_2$ . Spectra in the metallic (insulating) phase are indicated by full (dashed) lines in both (a) and (b).

in vanadium oxides<sup>14,34–36</sup> but also in various transition-metal oxides.<sup>37,38</sup> There is a small structure (labeled CT) located at around  $\sim 12$  eV above the main peak. This structure CT is ascribed to the charge-transfer satellite as clarified by cluster model calculations.<sup>34,35</sup> The V  $1s$  main peak in the insulating phase comprises two components in both  $V_5O_9$  and  $V_6O_{11}$  in contrast to a single component in the case of  $VO_2$  (Ref. 35) in the insulating phase. Although the relative intensity between the two components does not change much across MIT for  $V_5O_9$ , it changes much for  $V_6O_{11}$ , where the higher  $E_B$  component is noticeably suppressed above  $T_i$ .

Figure 3(b) summarizes the V  $2p$  core-level spectra. Both spectra in the metallic and insulating phases are normalized to have the same area of the V  $2p$  component after subtracting the integral backgrounds. On the lower  $E_B$  side of the V  $2p_{3/2}$  main peak, the well-screened final states labeled B are recognized in the metallic phase for all materials. The structure C, which is labeled on the lower  $E_B$  side of the V  $2p_{1/2}$ , may have the same origin. When the  $V_5O_9$  spectrum in the metallic phase is subtracted from the spectrum of metallic  $V_6O_{11}$ , it is clear that there is only little difference as shown by the empty circles at the bottom of Fig. 3(b). In the  $VO_2$  spectrum<sup>35</sup> in the insulating phase, the component B in the metallic phase is much suppressed and the intensity of the higher  $E_B$  component becomes suddenly stronger. A partly similar behavior is seen across MIT for  $V_6O_{11}$  while such a behavior is not obvious for  $V_5O_9$ . In the insulating phase, both  $V_5O_9$  and  $V_6O_{11}$  spectra show at least two components in contrast to a single component in  $VO_2$ . Moreover, the difference between the spectra of insulating  $V_5O_9$  and  $V_6O_{11}$  is clearly recognized. The spectral weight of the higher  $E_B$  component is larger than that of the lower  $E_B$  component in  $V_6O_{11}$  whereas the situation is opposite in  $V_5O_9$ . The vertical line drawn at  $\sim 515.8$  eV is a guide to the eye for comparison of the peak position in the  $2p$  spectra for  $V_5O_9$ ,  $V_6O_{11}$ , and  $VO_2$ .

In order to address these spectral behaviors mentioned above, we focus our attention on the difference in the distance between V ions. In the case of  $VO_2$  the V-V dimers are formed across the MIT with changing the value of the V-V distance from 2.85 Å (metallic phase) to 2.62 Å (insulating phase). As summarized in Table I,  $V_6O_{11}$  has six inequivalent

TABLE I. Distances between vanadium atoms (in the unit of Å). Values of  $V_5O_9(V_6O_{11})$  are from Marezio *et al.* (Ref. 24) [Schwingenschlögl *et al.* (Ref. 25)].

	$V_5O_9$		$V_6O_{11}$	
	Metallic (298 K)	Insulating (110 K)	Metallic (298 K)	Insulating (20 K)
V1-V2	3.50	3.50	2.77	2.77
V1-V3	2.96	2.95	2.95	2.90
V3-V5	2.82	2.81	2.91	2.99
V5-V5			2.80	2.79
V2-V4	3.04	3.00	2.95	3.06
V4-V6	2.89	2.95	2.85	2.62
V6-V6			2.82	3.30

vanadium sites and seven different V-V distances. One of them, namely, the shrinking of the V4-V6 distance in the insulating phase of  $V_6O_{11}$  corresponds to the V-V dimerization seen in  $VO_2$ , whereas the V-V distances for  $V_5O_9$  do not change so much.<sup>24</sup>

In order to clarify the origin of the different core-level line shapes among  $V_5O_9$ ,  $V_6O_{11}$ , and  $VO_2$  in the insulating phase, we try to reproduce the V  $1s$  and V  $2p$  core-level spectra of  $V_6O_{11}$  by a proper sum of the spectra of nondimerized  $V_5O_9$  and fully dimerized  $VO_2$  in the insulating phase. As shown in Fig. 4, the V  $1s(2p)$  spectrum of  $V_6O_{11}$  is well reproduced by the sum of the spectra of  $V_5O_9$  and  $VO_2$  with

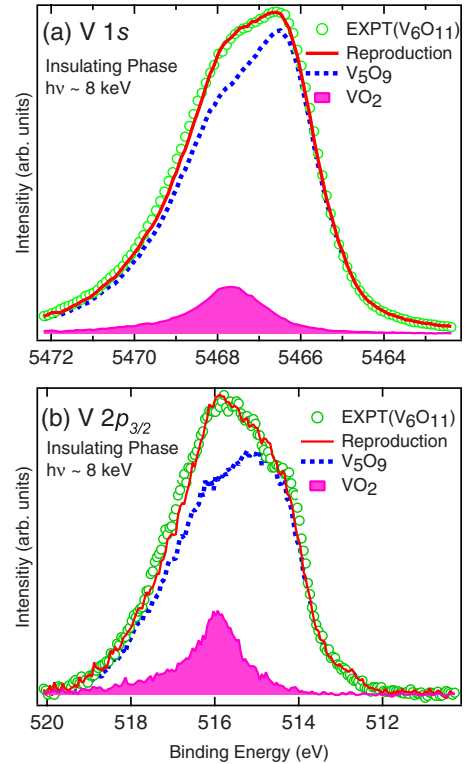


FIG. 4. (Color online). (a) V  $1s$  and (b) V  $2p_{3/2}$  spectra in the insulating phase of  $V_6O_{11}$  (open circles) can be reproduced by the sum of  $V_5O_9$  (dotted line) and  $VO_2$  (hatched area) data.



the ratio of  $\sim 90:10$  ( $\sim 85:15$ ). The fraction of the dimerized  $\text{VO}_2$  “contribution” in the reproduction process of  $\text{V } 2p_{3/2}$ , namely, 15%, is comparable to the ratio of the V4-V6 chains ( $\sim 17\%$ ) in the total V sites in the insulating  $\text{V}_6\text{O}_{11}$ . Therefore, we can conclude that the different core-level line shapes between  $\text{V}_5\text{O}_9$  and  $\text{V}_6\text{O}_{11}$  originate mainly from the contribution of the V-V dimerization in the insulating phase. Though the V-V dimerization effects cannot be observed clearly in the  $\text{V } 2p_{1/2}$  spectral weight for the insulating  $\text{V}_6\text{O}_{11}$ , we have confirmed that the  $\text{V } 2p_{1/2}$  spectral shape can be reproduced by the same procedure as for the  $\text{V } 2p_{3/2}$  spectra (not shown here).

On the other hand, rather similar spectral shapes are observed between  $\text{V}_5\text{O}_9$  and  $\text{V}_6\text{O}_{11}$  in the core-level spectra in the metallic phase as well as in the valence-band spectra in both metallic and insulating phases. The resemblance in the valence-band spectral shapes between these two compounds suggests that the strength of the electron correlation is comparable. Although the V-V dimerization effects are not so clear in the valence-band spectra of these materials compared with  $\text{VO}_2$ ,<sup>35</sup> they are explicitly traced in the core-level spectra. The relative spectral weight of the well-screened final states in the  $\text{V } 1s$  and  $2p$  core-level spectra in the metallic phase is stronger for  $\text{VO}_2$  than for these two materials, suggesting that the electron correlation effect is weaker for  $\text{VO}_2$ .

than for  $\text{V}_5\text{O}_9$  and  $\text{V}_6\text{O}_{11}$ . The MIT temperature  $T_i$ , on the other hand, is much higher for  $\text{VO}_2$  ( $\sim 340$  K for the bulk samples<sup>39</sup>). By further considering the facts that the antiferromagnetic ordering is seen at low temperatures in insulating phase of  $\text{V}_5\text{O}_9$  and  $\text{V}_6\text{O}_{11}$  while  $\text{VO}_2$  is nonmagnetic below  $T_i$  (Ref. 18) in addition to our spectroscopic results, we conclude that the mechanism of MIT for  $\text{V}_5\text{O}_9$  and  $\text{V}_6\text{O}_{11}$  is much different from that for  $\text{VO}_2$ . Still it is unclear whether that for  $\text{V}_5\text{O}_9$  and  $\text{V}_6\text{O}_{11}$  is similar to  $\text{V}_2\text{O}_3$ .

In conclusion, we have performed HAXPES for the Magnéli phase  $\text{V}_5\text{O}_9$  and  $\text{V}_6\text{O}_{11}$ . The valence-band spectra show similar spectral shapes for  $\text{V}_5\text{O}_9$  and  $\text{V}_6\text{O}_{11}$  in both metallic and insulating phases, suggesting comparable electron correlation effects. The core-level spectra in the insulating phase, however, differ clearly between them, reflecting the effects of the partial V-V dimerization effects in  $\text{V}_6\text{O}_{11}$ . The mechanisms of the MIT for  $\text{V}_5\text{O}_9$  and  $\text{V}_6\text{O}_{11}$  is different from that for  $\text{VO}_2$ .

We would like to thank A. Yamasaki, H. Fujiwara, and G. Funabashi for supporting the experiments. This work was supported by Grant-in-Aid for Scientific Research (Grants No. 15G0213, No. 18104007, and No. 18684015) of MEXT and Global COE program (G10) of JSPS, Japan, and the KHYS of the Karlsruhe Institute of Technology.

\*Present address: Graduate School of Science and Engineering, Ritsumeikan University, 1-1-1 Noji Higashi, Kusatsu, Shiga 525-8577, Japan.

- <sup>1</sup>J. P. Pouget, H. Launois, T. M. Rice, P. Dernier, A. Gossard, G. Villeneuve, and P. Hagenmuller, *Phys. Rev. B* **10**, 1801 (1974).
- <sup>2</sup>D. B. McWhan, T. M. Rice, and J. P. Remeika, *Phys. Rev. Lett.* **23**, 1384 (1969).
- <sup>3</sup>R. M. Moon *et al.*, *Phys. Rev. Lett.* **25**, 527 (1970).
- <sup>4</sup>P. D. Dernier *et al.*, *J. Phys. Chem. Solids* **31**, 2569 (1970).
- <sup>5</sup>D. B. McWhan, A. Menth, J. P. Remeika, W. F. Brinkman, and T. M. Rice, *Phys. Rev. B* **7**, 1920 (1973).
- <sup>6</sup>N. F. Mott *et al.*, *Rev. Mod. Phys.* **40**, 677 (1968).
- <sup>7</sup>D. Adler and H. Brooks, *Phys. Rev.* **155**, 826 (1967).
- <sup>8</sup>R. M. Wentzcovitch, W. W. Schulz, and P. B. Allen, *Phys. Rev. Lett.* **72**, 3389 (1994).
- <sup>9</sup>A. Zylbersztejn and N. F. Mott, *Phys. Rev. B* **11**, 4383 (1975).
- <sup>10</sup>S. Shin, S. Suga, M. Taniguchi, M. Fujisawa, H. Kanzaki, A. Fujimori, H. Daimon, Y. Ueda, K. Kosuge, and S. Kachi, *Phys. Rev. B* **41**, 4993 (1990).
- <sup>11</sup>T. M. Rice, H. Launois, and J. P. Pouget, *Phys. Rev. Lett.* **73**, 3042 (1994).
- <sup>12</sup>K. Okazaki, A. Fujimori, and M. Onoda, *J. Phys. Soc. Jpn.* **71**, 822 (2002).
- <sup>13</sup>S. Biermann, A. Poteryaev, A. I. Lichtenstein, and A. Georges, *Phys. Rev. Lett.* **94**, 026404 (2005).
- <sup>14</sup>R. Eguchi *et al.*, *Phys. Rev. B* **78**, 075115 (2008).
- <sup>15</sup>P. C. Canfield, J. D. Thompson, and G. Gruner, *Phys. Rev. B* **41**, 4850 (1990).
- <sup>16</sup>H. Horiuchi *et al.*, *J. Solid State Chem.* **17**, 407 (1976).
- <sup>17</sup>H. Katzke, P. Tolédano, and W. Depmeier, *Phys. Rev. B* **68**, 024109 (2003).
- <sup>18</sup>U. Schwingenschlögl *et al.*, *Ann. Phys.* **13**, 475 (2004).

- <sup>19</sup>S. Hüfner, *Photoelectron Spectroscopy* (Springer-Verlag, Berlin, 2003).
- <sup>20</sup>A. Sekiyama *et al.*, *Nature (London)* **403**, 396 (2000).
- <sup>21</sup>S. Suga *et al.*, *J. Phys. Soc. Jpn.* **74**, 2880 (2005).
- <sup>22</sup>A. Yamasaki *et al.*, *Phys. Rev. Lett.* **98**, 156402 (2007).
- <sup>23</sup>M. Yano *et al.*, *Phys. Rev. B* **77**, 035118 (2008).
- <sup>24</sup>M. Marezio *et al.*, *J. Solid State Chem.* **11**, 301 (1974).
- <sup>25</sup>U. Schwingenschlögl *et al.*, *Europhys. Lett.* **61**, 361 (2003).
- <sup>26</sup>K. Nagasawa, Y. Bando, and T. Takada, *J. Cryst. Growth* **17**, 143 (1972).
- <sup>27</sup>S. Suga and A. Sekiyama, *Eur. Phys. J. Spec. Top.* **169**, 227 (2009).
- <sup>28</sup>K. Nagasawa *et al.*, *Jpn. J. Appl. Phys.* **9**, 407 (1970).
- <sup>29</sup>H. Okinaka *et al.*, *J. Phys. Soc. Jpn.* **28**, 803 (1970).
- <sup>30</sup>H. V. Keer *et al.*, *J. Phys. C* **10**, L637 (1977).
- <sup>31</sup>The bulk incoherent part is much more clearly seen in HAXPES spectra of  $\text{V}_4\text{O}_7$  and  $\text{V}_2\text{O}_3$  [H. Fujiwara, A. Sekiyama, S.-K. Mo, J. W. Allen, J. Yamaguchi, G. Funabashi, S. Imada, P. Metcalf, A. Higashiya, M. Yabashi, K. Tamasaku, T. Ishikawa, and S. Suga, arXiv:0908.2870 (unpublished)].
- <sup>32</sup>E. Pavarini, S. Biermann, A. Poteryaev, A. I. Lichtenstein, A. Georges, and O. K. Andersen, *Phys. Rev. Lett.* **92**, 176403 (2004).
- <sup>33</sup>R. J. O. Mossaneck and M. Abbate, *Phys. Rev. B* **75**, 115110 (2007).
- <sup>34</sup>N. Kamakura *et al.*, *Europhys. Lett.* **68**, 557 (2004).
- <sup>35</sup>S. Suga *et al.*, *New J. Phys.* **11**, 103015 (2009).
- <sup>36</sup>G. Panaccione *et al.*, *Phys. Rev. Lett.* **97**, 116401 (2006).
- <sup>37</sup>K. Horiba *et al.*, *Phys. Rev. Lett.* **93**, 236401 (2004).
- <sup>38</sup>M. Taguchi *et al.*, *Phys. Rev. Lett.* **95**, 177002 (2005).
- <sup>39</sup>K. Nagashima *et al.*, *J. Appl. Phys.* **101**, 026103 (2007).